

DOUBLE TRANSFER EXPERIMENTS TO HIGHLIGHT DESIGN CRITERION FOR FUTURE SELF-LUBRICATING MATERIALS

G. COLAS ^(1,2), A. SAULOT ⁽²⁾, S. DESCARTES ⁽²⁾, Y. MICHEL ⁽³⁾, Y. BERTHIER ⁽²⁾

⁽¹⁾ University of Toronto, Department of Mechanical and Industrial Engineering, 5 King's College Road, Toronto, ON M5S3G8, Canada E-mail: guillaume.colas@utoronto.ca

⁽²⁾ INSA de Lyon, LaMCoS UMR CNRS 5259, 18-20 rue des Science, 69621 Villeurbanne, France E-mail: aurelien.saulot@insa-lyon.fr, sylvie.descartes@insa-lyon.fr, yves.berthier@insa-lyon.fr,

⁽³⁾ CNES, 18 avenue Edouard Belin, 31401 Toulouse Cedex 9 E-mail: yann.michel@cnes.fr

ABSTRACT

Following the cessation of the Duroïd 5813 manufacturing, PGM-HT has been identified as the best candidate to replace it as the self-lubricating material for space application. However, discussions remain on its performances. Moreover, PGM-HT is an US product with no possibility to provision core material which makes it difficult for Europe to fully have the required knowledge to fit material to applications or vice-versa. Consequently, it is necessary to develop new material on the European side.

The present study aims to complement the numerous ongoing studies which mainly investigate self-lubricating materials on Pin-On-Disc or bearing testers. A specific tribometer has thus been designed along with its associated tribological analysis.

Results notably highlight some underlying role of the fibers and the associated size effect in trapping lubricious materials in the contact and in controlling the tribological properties of the transfer films, and consequently the lubrication.

1 INTRODUCTION

Following the cessation of the Duroïd 5813 manufacturing, PGM-HT has been identified by ESTL and ESA as the best candidate to replace it as the self-lubricating material for space application, providing some specific requirements on its fabrication and use [1,2]. However, discussions remain on its lubrication performances in ball bearings, especially on its capability to transfer material on both the balls and the races without damaging them to ensure good lubrication [3,4]. To avoid lubrication failure, it has been recommended to coat both the balls and the races with MoS₂ [2].

Consequently, the uncertainties and limitations, plus the secrecy around the PGM-HT urge the development of new material on European side. Numerous studies at ESTL, AAC, CNES and ESA either were or are still on-going. They mainly investigate the materials on Pin-On-Disc or bearing testers [1,3-5] and compare the performances of

materials (friction coefficient and wear) depending on the nature of their constituents using PGM-HT and Duroïd as references. From Pin-On-Disc to bearing a big gap exist due the differences in the emulated kinematics. Consequently, on CNES-LaMCoS side, it has been decided to develop a double transfer test bench (DTTB) to study more fundamentally the double transfer mechanisms encountered in the dry lubrication of ball-bearing. The aim is to highlight more quantitative criterions to test/validate and ideally design new materials.

2 EXPERIMENTAL DETAILS

2.1 The Double Transfer Test Bench (DTTB)

The DTTB (Figure 1) can simulate both retainer/ball and ball/race contacts. It is mounted in an environmental chamber equipped with force sensors, and a mass spectrometer to track the consumption of the composite material during the test.

The bearing is simulated with 3 samples:

- A barrel shaped ball (Ø 25mm, roundness Ø 1000mm) whose motion is only rotation,
- A flat plate sample (l = 109mm, w = 10mm, t = 14mm) whose motion is only translation,
- A cylindrical pad sample (Ø 8mm) made of the composite to be tested to emulate the retainer.

The ball can be in contact with the retainer only or with both the retainer and the plate. The sample simulating the retainer is mounted on a sensor measuring the force F1 with a sensitivity of ±0.01 N. The sensor allows monitoring the variations of the load all along the test. The contact load F1 between the sample simulating the retainer and the ball, is applied via two compression springs. The assembly is guided in the support thanks to two roller guides. As it is shown in Figure 1, the assembly is a long suspended structure that gives the freedom to its end (basically the surface in contact with the ball) to slightly move around its center position. Such freedom was chosen as the contact between the ball and the retainer in a bearing is far from being rigidly

fixed. The literature [7] shows that the degrees of freedom of the system applying the contact conditions have a big impact on the creation and the distribution of the 3rd body inside the contact. The 3rd body is essentially composed of the particles detached from the materials initially in contact (called 1st bodies) and circulating inside the contact. Here the 3rd body is eventually becoming the transfer films on both balls and races, and it carries loads and accommodates velocity at the contact.

Consequently, the DTTB and the associated analysis will help to understand the 3rd body creation, its circulation inside the contact and ultimately its arrangement to form the transfer film. In other words, such global understanding approach will help understand the friction and wear processes governing the double transfer lubrication, and consequently the associated tribological behavior observed in mechanisms.

2.2 Materials

8 materials are studied. Among them, 5 are commercially available:

- PGM-HT (PTFE matrix, MoS₂ Ø100µm, glass fiber Ø20µm), produced by JPM Mississippi (USA). The PGM-HT was pre-conditioned in vacuum.
- 4 Tecasint produced by Ensinger (Europe):
 - 1041 (Polyimide (PI) matrix, 30% MoS₂),
 - 4041 (PI matrix, 30% MoS₂),
 - 8001 (PTFE matrix, 20% PI) and 8061 (PTFE matrix, 40% PI),
- 2 materials developed by AAC under ESA contract.
 - C1 (PTFE matrix, MoS₂, glass fiber),
 - C9 (PTFE, MoS₂, mineral fiber),

- Duroïd 5813(PTFE matrix, MoS₂ Ø10µm, glass fiber Ø3µm) whose production ceased few decades ago is also tested. It was originally produced by Rogers Corp. (USA).

C1 and C9 are the result of a previous study where several materials were tested in different conditions to identify the key to the most promising formulation [5]. Some data cannot be disclosed, especially for C1 and C9, it can only be said that the diameter of the fibers are from the smallest to the highest Duroïd < C9 < C1 < PGM-HT. For MoS₂ particles, the order is Duroïd < C9 = C1 < PGM-HT.

The ball and plate samples are made of AISI440C with a roughness Ra < 0.1 µm. Prior to experiments, samples are cleaned with respect to a protocol developed by CNES [6]. Composite samples are machined with respect to the machining process of the real bearing retainers to get a similar surface finish. Roughness is not given here as particles stay stuck or can be loosely embedded at the surface of the material after machining.

Finally, no MoS₂ coatings are deposited on samples in order to study only the capability of the materials to double transfer on the ball and on the race.

2.3 Contact conditions

The kinematic is an alternative motion to reproduce the motion of ball bearing in a real mechanism. The displacement amplitude of the plate sample is 75 mm in total which covers approximately 95% of the roller perimeter. The linear speed of the ball is 100mm/s and representative of classic space mechanisms' bearings such as the STD and Polder mechanism used by CNES in a former study [4].

Contact loads are 1.5 N at the contact retainer/ball (around 10 MPa of max Hertz theoretical initial contact pressure) and 125 N at the contact ball/race (0.5 GPa of max Hertz contact pressure for this first

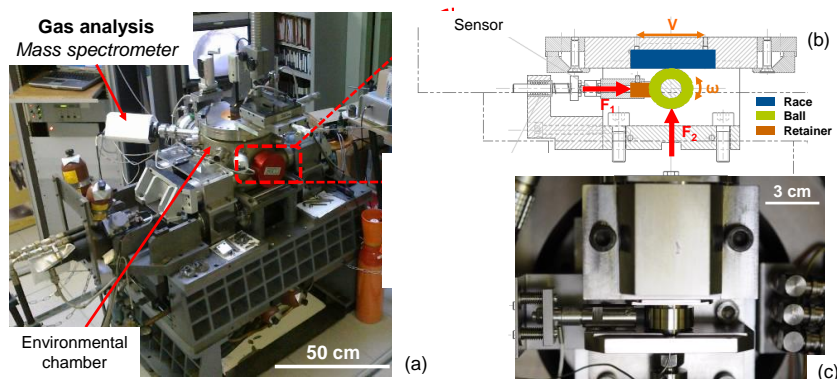


Figure 1 - Double Transfer Test Bench (DTTB): (a) full tribometer; (b) cross section view of the DTTB ; (c) top view of the contact between the retainer and the ball

set of experiment). Experiments are conducted in UHV (10^{-7} mbar) and in air 50%HR. Experiments are done in 3 phases of 5000 cycles each to emulate different working conditions:

- A- Running in with only the ball/retainer contact to emulate the gentle run in
- B- Rolling without sliding with both ball/retainer and ball/race contacts to emulate ideal working conditions
- C- Rolling with 0.5% sliding with both contacts to emulate severe working conditions

To understand what happens at each steps, some materials can see only the phase A or the phases A & B. Experiments containing only phase A allow top view visualization of the ball. Consequently, a video camera is used to study the friction track on the ball.

3 RESULTS

The results will focus on the variations of the normal load F1 at the contact between the retainer and the ball and on the post-test analysis conducted on the different samples. For the UHV experiments, data obtained from the mass spectrometry will also be taken into considerations. Finally, no wear rates have been reported by choice as it appears meaningless for the study as it will be shown all along the section.

The reason for considering only the variations of the normal load F1 at the contact relies on the fact that it is the only one that really allows to discriminate the materials. Indeed, the current consumption by the motor is approximately the same for each materials, as well as the tangential force measured at the contact between the ball and the plate. For the latter, the measured force is extremely low (close to the lower limit of measuring range) due to the rolling

motion. A significant increase implies high adhesion, if not cold-welding, at the contact, i.e. failure of lubrication. The significant events such as big particle formation, increase in motor torque noise (related to current consumption), are strongly amplified in the normal load F1. Consequently, F1 efficiently helps to discriminate the materials and link their behavior to both the composite and the 3rd body constitutions, morphology, etc. Those are studied with SEM and EDS after the test. The evaluation of both the transfer capabilities of materials and the 3rd body morphology is qualitative.

Table 1 to 4 display the optical microscope images of the pad emulating the retainer and the plates emulating the race for each composites after a UHV test containing the 3 phases. As it can be seen, the double transfer is successfully emulated. The ball exhibit the same morphologies than the counter plate. Table 1 to 4 also display the mean friction coefficient measured in phase A.

3.1 Experiments in UHV

For composites made of 3 components and from the optical images (Table 1), in terms of transfer capabilities and particle generation, the qualitative evaluation shows that:

- PGM-HT transfers a little but produces a lot of particles. An important volume can be detected around the contact ellipse on the pad,
- Duroïd transfers a little more than the PGM-HT but produces a slightly lower amount of particles. Those particles can be easily detected around the contact ellipse on the pad and a few can be seen around the

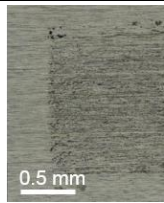
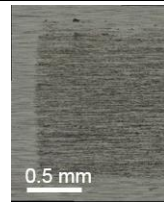
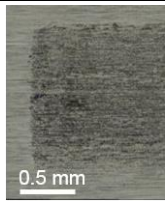
	PGM-HT	Duroïd 5813	C1	C9
Pad				
Plate				
$\mu(A)$	0.2	0.3	0.27	0.25

Table 1 - Optical microscope images of PGM-HT, Duroïd, C1 and C9 after a test composed of the 3 phases with the associated friction coefficient in phase A (ball/retainer contact). in UHV

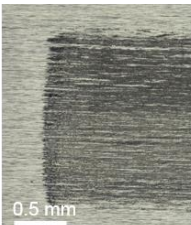
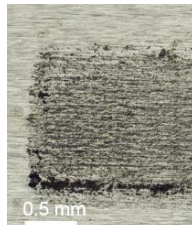
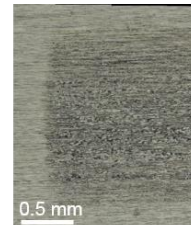
	Tecasint 1041	Tecasint 4041	Tecasint 8001	Tecasint 8061
Pad				
Plate				
$\mu(A)$	0.4	0.2	0.3	0.23

Table 2 - Optical microscope images of the Tecasint materials after a test composed of the 3 phases with the associated friction coefficient in phase A (ball/retainer contact). In UHV

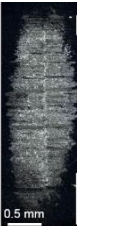
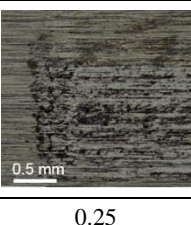
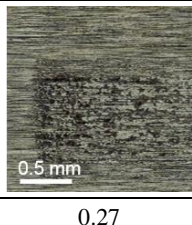
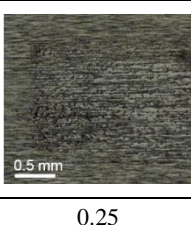
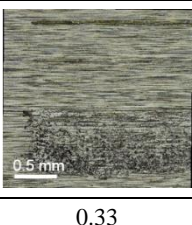
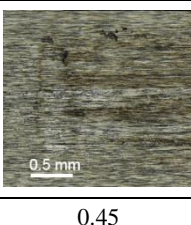
	PGM-HT	Duroïd 5813	C1	C9	T.4041
Pad					
Plate					
$\mu(A)$	0.25	0.27	0.25	0.33	0.45

Table 3 - Optical microscope images of the materials after a test composed of the 3 phases with the associated friction coefficient in phase A (ball/retainer contact). In air 50%HR

friction track on the plate,

- C1 transfers a little more than the Duroïd and produces a significantly lower amount of particles. Those particles can be detected around the contact ellipse on the pad and a few can be seen around the friction track on the plate,
- C9 transfers a little more than C1 but produces a higher amount of particles. The amount is close to what was observed with Duroïd. Those particles can be detected around the contact ellipse on the pad and a few can be seen in and around the friction track on the plate.

For composites made of 2 components, i.e. the Tecasint, and from the optical images (Table 2), in terms of transfer capabilities and particle generation:

- 1041 transfers significantly. Indeed, a thick homogeneous 3rd body layer is detected on the plate. Moreover, contrary to the 3 component composites, particles are detected on neither the pad nor the plate where the contact ellipse is very smooth,
- 4041 also transfers significantly but the 3rd body layer formed is not as homogeneous as it is with 1041. Contrary to 1041, 4041 produces an amount of particles close to what is produced with Duroïd. Those particles can be easily detected around and inside the contact ellipse on the pad and a significant amount (compared to the other materials) can be seen around and inside the friction track on the plate,
- 8001 transfers less materials than both 1041 and 4041. However the transfer appears equivalent to what is detected with PGM-HT. Similarly to 1041,

particles are detected on neither the pad nor the plate where the contact ellipse is very smooth,
 - 8061, like 8001, transfers less materials than both 1041 and 4041. However the transfer appears equivalent to what is detected with Duroïd. Similarly to 1041, particles are detected on neither the pad nor the plate where the contact ellipse is very smooth.

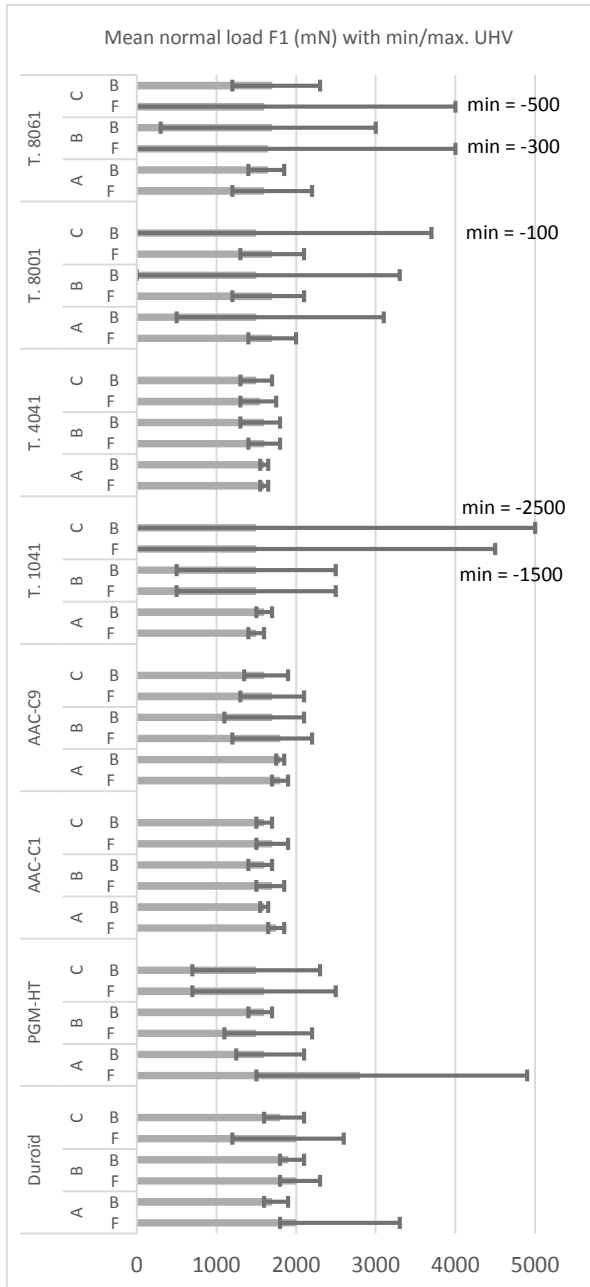


Figure 2 - Mean F1 load with its min and max (contact retainer/ball) during the friction test in UHV. F = Forward motion and B = Backward motion.

In term of friction coefficient, as it shown in Tables 1 to 3, the friction coefficient in phase A (retainer/ball contact) mainly stays in the 0.2 to 0.3 range, apart for the Tecasint 1041 in UHV and the Tecasint 4041 in air.

Regarding the variations of the normal load F1 at the retainer/ball contact (Figure 2), the best behavior is obtained with the composite C1, followed by the Tecasint 4041, C9, Duroïd and finally PGM-HT. Indeed, they exhibit a very low noise. It has to be noted that the high maximum value detected in phase A, forward motion F, for both PGM-HT and Duroïd is due to the circulation of big 3rd body particle inside the contact (Figure 3). To the contrary, the noise detected with the composites Tecasint 1041, 8001 and 8061 are due to instabilities inside the contact that put the contact in vibrational state. During the experiment, a typical sound is emitted by the contact when it enters into that state. It is interesting to note that the material giving the most unstable behavior is the one producing the thickest and most homogeneous transfer film, i.e. Tecasint 1041. The morphology of the transfer films appears highly cohesive and adhesive. To the contrary, the material exhibiting the most stable behaviors are the materials showing 3rd body particles creation.

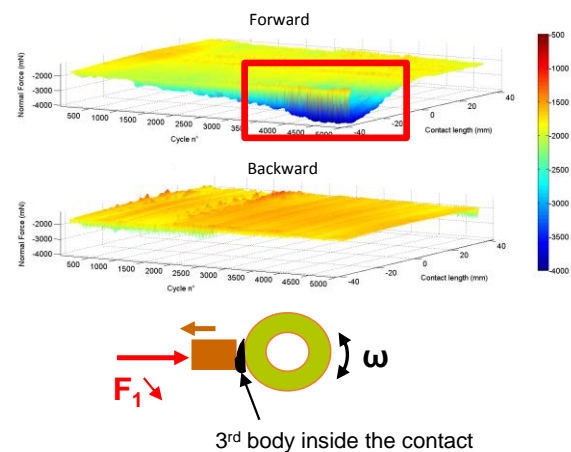


Figure 3 - Impact of 3rd body big particle circulating inside the pad/ball contact: compression of the sensor inducing an increase in the absolute value of the force. Curve from PGM-HT, F1 in mN.

To have a better insight of the particle creation and distribution around and inside both the contact ellipse and the plate, samples were observed with a SEM. As shown on Figure 4, a significant amount of 3rd body particles is trapped inside the friction track thanks to the glass fibers in the case of the composites made of 3 components (PGM-HT, Duroïd, C1 and C9). A much lower amount is detected inside the contact ellipse of the Tecasint 1041, 8001 and 8061. The case of the Tecasint 4041 is still under investigation.

Nonetheless, 3 components composites exhibit a significant amount of free 3rd body inside the contact ellipse. The 3rd body is a powdery material composed of a mix of PTFE, MoS₂ and fragmented glass fibers.

Depending on its location it can be more or less compacted. On the plate, the transferred 3rd body layer exhibits a compacted morphology with ductile properties while the particles are still powdery. It has to be noted that such morphology has been seen in former inspected bearings (Figure 6) operated in real conditions. This shows the relevance of the study.

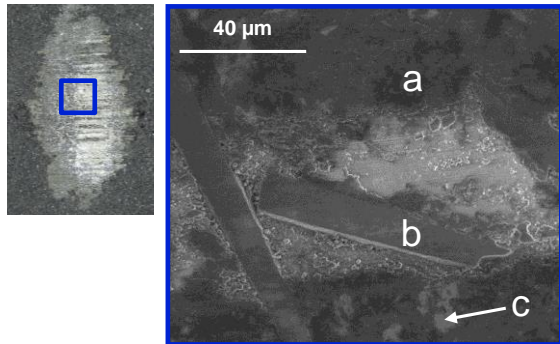


Figure 4 - SEM image of pad sample from PGM-HT after 3 phase friction test in UHV. a: 3rd body (PTFE, MoS₂, fiber) ; b: fiber ; c: MoS₂

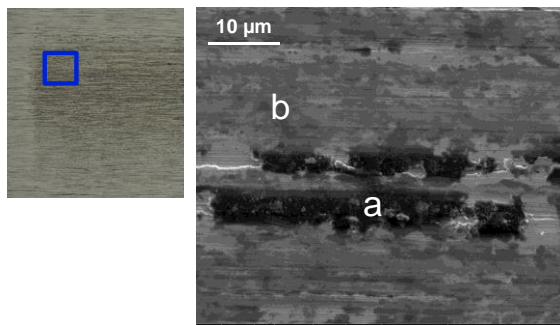


Figure 5 - SEM image of plate sample from PGM-HT after 3 phase friction test in UHV. a: granular 3rd body; b: compacted thin 3rd body layer

It is difficult to link the size of the particle constituting the powdery 3rd body to the initial size of the fibers and MoS₂ particles. Indeed, as soon as a fiber detaches from the bulk, before being fragmented into pieces, it can circulate inside the contact and induce high loads as seen on Figure 2 with PGM-HT. The sizing of the fibers must play a role in its adhesion/cohesion to the matrix as the fiber can be sheared in half (Figure 4). However, once all detached pieces are broken into tiny pieces, the resulting size appears to be equivalent for all composite materials. Finally, on some samples, the EDS analysis showed the presence of Fe in the contact area on the pad, especially for PGM-HT. This tends to agree with the literature [4,8], the fiber size might influence the scratching of the metallic counterparts and the particle detachment from them.

To the contrary, the 3rd body created with the unstable Tecasint (1041, 8001 and 8061) have less

mobility and appears less powdery. Indeed, only a few free isolated particles are detected (Figure 7).

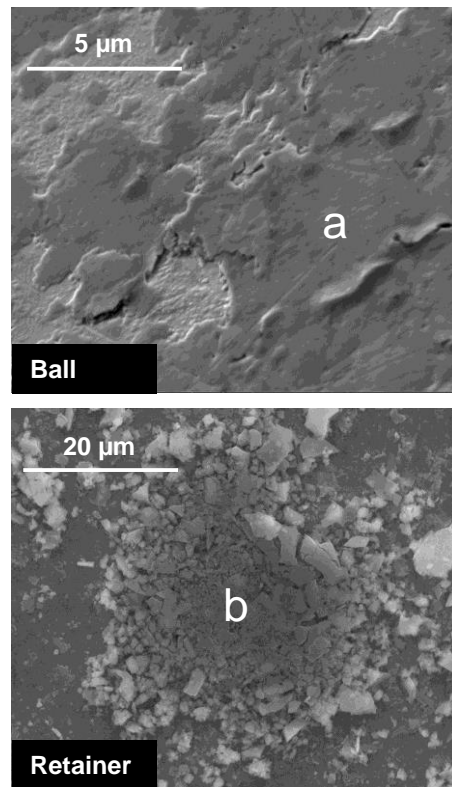


Figure 6 - SEM images from a ball bearing lubricated with PGM-HT only. a: 3rd body layer on the ball; b: 3rd body on the retainer at the ball/retainer contact

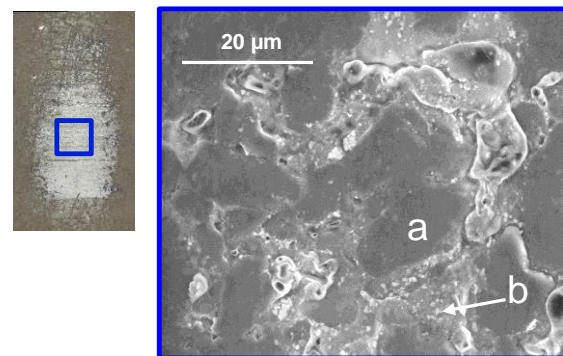


Figure 7 - SEM image of pad sample from Tecasint 8061 after 3 phase friction test in UHV. a: Polyimide (PI) inclusion; b: isolated 3rd body particle.

Finally the mass spectrometry, via the detection of HF and C₂F₄, shows that the composite Duroïd and PGM-HT tends to be mainly consumed at the beginning of each phase during a defined period while C1 and C9 appears to be consumed or stressed all along the test. The observation, at naked eyes through a window of the chamber, shows that Duroïd transfers materials poorly in phase A (almost no material is seen on the ball, only few patches), slightly better in phase B (some patches appears), and fairly well in phase C (Table 1). PGM-HT

transfers poorly in phase A but fairly well in both phase B and C. C9 shows the same tendencies than PGM-HT. C1, as well as Tecasint 4041, show the best behaviors with fairly good transfer in both phase A and B, and a good transfer capability in phase C. The increase of transfer in phase B and then C can be due to the natural response of the contact to higher stresses by demanding more 3rd body material to help carrying the loads and accommodate velocities. But physically, the increase of transfer might be due to higher activation of the surfaces which would facilitates the bounding of the 3rd body to the metallic counterparts and the building of the 3rd body layer known as transfer film.

The mass spectra obtained during the tests conducted with the Tecasint show that they appear to be consumed and/or stressed all along the test too. Such indication is consistent with what is seen in terms of transfer capability of Tecasint 4041. However, it is interesting to note that Tecasint 1041 transfers nothing during phase A but then transfers fairly well in phase B and a lot in phase C. Tecasint 8001 appears close to the PGM-HT in term of transfer while Tecasint 8061 is closer to Duroïd.

3.2 Experiments in Air, 50% HR

Only the materials that successfully passed the vacuum tests were chosen to undergo the tests in air. Consequently, only Duroïd, PGM-HT, C1, C9 and Tecasint 4041 were tested in air.

From Table 3, it can be stated that all material successfully transferred materials to the plate, i.e. that the double transfer is effective. However, compared to what was observed in UHV, the transfer is coarser with bigger 3rd body patches on the plate for Duroïd, PGM-HT, C1, and C9. Regarding the Tecasint 4041, the transfer film appears thinner and less coarse than what was observed in UHV. Finally, the friction coefficient in phase A is much higher than it was in UHV for Tecasint 4041.

In terms of particle creation, Duroïd, PGM-HT, C1, and C9 exhibit a big amount of particles, slightly bigger than what was observed in UHV. Dark field images shows a brown/orange colored 3rd body consistent with MoS₂ oxidization. To the contrary, Tecasint 4041 exhibits no particles and a smooth contact ellipse on the pad. That smoothness is very similar to the morphologies observed for the other Tecasint after the friction test conducted in UHV.

As shown on Figure 8, the only material exhibiting unstable behavior is the Tecasint 4041. The other

materials exhibit a very stable behavior with very low variations of the normal load F1 at the retainer/ball contact. Between those 4, the best material, in terms of F1 stability, is C9, equally followed by Duroïd and C1, and then PGM-HT.

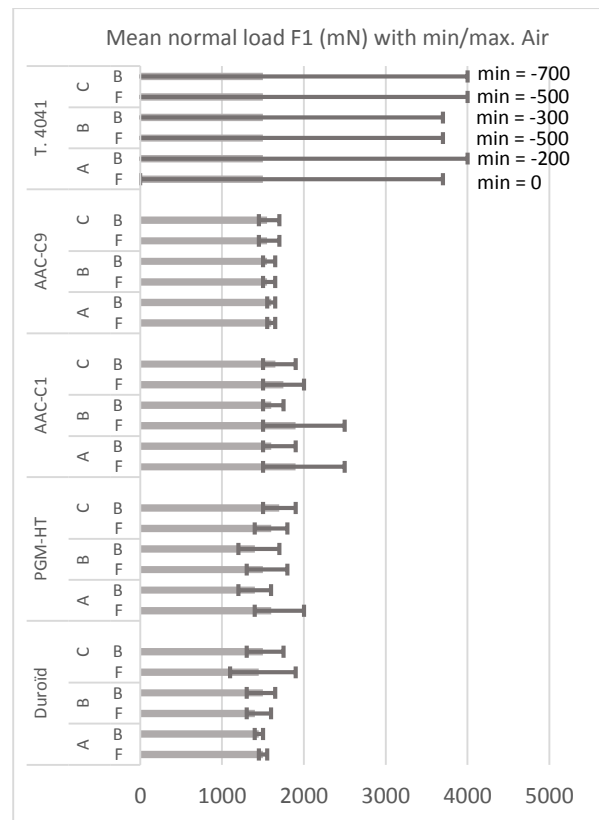


Figure 8 - Mean F1 load with its min and max (contact retainer/ball) during the friction test in Air. F = Forward motion and B = Backward motion.

The samples are currently still under investigation under SEM to clearly establish the differences in the 3rd body morphology between the one obtained in UHV and the one obtained in air. There is no mass spectrometry information as the mass spectrometer mounted on the environmental chamber can only work in vacuum.

4 DISCUSSION & CONCLUSIONS

Results showed successful capability of the DTTB to reproduce the double transfer lubrication occurring in real mechanisms. Indeed, the double transfer occurred and the created 3rd body materials had the same morphologies than those created in a real ball bearing solely lubricated by composite. No coatings were deposited on the races and the balls. The results particularly showed that relying only on the evaluation of the double transfer capability, or on the friction coefficient between composite materials and a single counter-material, may lead to wrong conclusions. Indeed, it has been shown in UHV that the composite transferring the most (Tecasint 1041)

is also the one exhibiting the most unstable behavior. Similarly, two materials exhibiting the same friction coefficient (Duroïd and Tecasint 8001 in UHV) can exhibit totally different tribological behaviors.

Secondly, the fillers and especially fibers are showed to control both the trapping of 3rd body particles needed to form the transfer film and the film's cohesion. They consequently greatly influence the noise observed in the force measurements and take actively part in the lubrication process. However, they also influence the occurrence of scratches and material detachment from the metallic counter parts. Although it has to be confirmed, it appears that a limit size exists above which both scratches of the counterpart occurs and created 3rd body particles are initially big enough to disturb the contact. Concerning, their distribution inside the composite, the literature [8] appears to show that chopped fibers homogeneously distributed in random directions appears to be the best. The results of the present study do not allow to conclude on it as no composite shows evenly distributed and oriented fibers.

Then, the study showed that a stable behavior is only obtained when the 3rd body exhibit a certain freedom of circulation inside the contact ellipse while the transferred film shows some ductility. The very smooth morphology of the contact ellipse on the pad appears very consistent with the unstable tribological behavior in both UHV (Tecasint 1041, 8001, 8061) and air (Tecasint 4041). Consequently, efficient lubrication appears to be obtained when a "mobile" powdery 3rd body is created in the retainer/ball contact but is trapped inside the contact thanks to the fibers. Then once transferred, it is spread and compacted to form a layer plastically deformable to transmit contact loads and accommodate velocities. The tiny particles created by the rupture of the fibers might play a role in the cohesion of that layer and its adhesion to other surfaces. No wear rates have been reported by choice as it appears meaningless for the study. The authors chose the definition of wear from the 3rd body concept stating that wear defines the 3rd body definitely ejected outside the contact. The 3rd body circulating inside the contact is actively taking part in the lubrication and consequently in the control of the composite consumption. When the required 3rd body is created, particle detachment from the materials stops.

Finally, the results show that AAC and ESA go in the right direction in the development of future self-lubricating materials. Indeed, the composites C1 and C9 exhibit the best performances in both UHV and air 50%HR.

5 FUTURE WORK

To confirm the results and go further in the study, component level tests have just started with ball

bearing lubricated only with PGM-HT, Duroïd, C1 and C9. Moreover, all the results are used to inform a DEM code currently under development. The aim is to model the creation of the transfer film from the detachment of particle to allow an easier parametric study on the role of the different fillers in term of size, distribution, orientation, mechanical properties, etc.

6 ACKNOWLEDGEMENTS

The authors would like to thank CNES for supporting the study. They also thank Andreas Merstallinger from AAC for providing the composites C1 and C9 samples and for taking part to the discussions on the results. The authors thank Tatiana Quercia for her help in the observation of the samples and Prof. Tobin Filleter for his help in reviewing the paper.

7 REFERENCES

1. Anderson, M.J. (1999). Tribometer characterisation tests and definition of bearings screening plan. ESA-ESTL-TM-226 01-
2. Palladino, M. (2012). Report on ESA recommendations regarding PGM-HT use for space applications. ESA/ESTEC/TEC-MSM/2012/111/ln/MP
3. Buttery, M. Cropper, M. Roberts, E.W. (2011). Thermally conditioned PGM-HT. ESA-ESTL-TM-0069
4. Sicre, J. Michel, Y. Videira, E. Nicollet, L. Baud, D. (2009). PGM-HT as RT/Duroïd 5813 replacement? Lifetime results on STD Earth scanning sensor and Polder bearing shaft. 13th ESMATS, ESA-SP-670, July 2009
5. Macho, C. Merstallinger, A. Brodowski-Hanemann, G. Palladino, M. Pambaguian, L. (2013). SLP_{MC} – Self Lubricating Polymer Matrix Composites. 15th ESMATS, ESA-SP-718, September 2013
6. Cordier, C. Procédure de nettoyage de pieces mécaniques, métalliques, plastiques, composites ou céramiques appliqué au laboratoire de DCT/TV/MS. DCT-TV-MS-2009-6283-1.0, CNES, 2009
7. Berthier, Y. (1992) Tribologie – Sciences Carrefour. Journée Européenne du Freinage J.E.F.92, Lille
8. Martin, Ch. Sailleau, J. Pesenti, P. (1974) Expérimentation des composites autolubrifiants pour roulements spatiaux. In : CNES (Editors), La Recherche Spatiale (13) 20-24